

Continuous real-time measurement of fluorescence lifetimes

W. Trabesinger,^{a)} C. G. Hübner, B. Hecht,^{b)} and U. P. Wild
*Physical Chemistry Laboratory, Swiss Federal Institute of Technology, ETH-Hönggerberg,
CH-8093 Zürich, Switzerland*

(Received 25 March 2002; accepted for publication 6 May 2002)

We report on the continuous measurement of fluorescence lifetimes at low light levels. Fluorescence photons following pulsed excitation generate a pulse sequence with exponentially distributed amplitudes and interphoton times at the output of a time-to-amplitude converter. This sequence is turned into a continuous step function and is time averaged with an adjustable bandwidth. For a single-exponential decay, our approach yields identical results as would be obtained from fitting fluorescence decays, while being a real-time technique. The proposed technique performs especially well at low count rates. We demonstrate the applicability of the method at the example of confocal fluorescence lifetime imaging of single molecules. © 2002 American Institute of Physics.
[DOI: 10.1063/1.1488676]

Optical microscopy of fluorescent samples relies on the spatially resolved measurement of intensity and other spectroscopic parameters. For example, the excited state lifetime of fluorescent molecules is often of particular interest, since it is both intensity independent and sensitive to changes in the environment of the fluorophore.¹ Most commonly, fluorescence lifetimes are measured using so-called time-correlated single-photon counting (TCSPC).² In TCSPC, the time lag between an excitation laser pulse and the emission of a fluorescence photon is measured for many individual photons. Combination of these time lags into a histogram and subsequent fitting of the latter with an exponential decay allows for accurately determining the fluorescence lifetime. However, the time-consuming process of fitting exponential decays prohibits the use of TCSPC in time-critical applications. A well-known approach to the real-time measurement of fluorescence lifetimes is based on modulating the excitation laser light and detecting the phase-shifted fluorescence. The magnitude of the phase shift depends on the excited state lifetime.³ As this method is based on lock-in techniques, it is restricted to strong fluorescence signals and analog detectors. In many fields of science and technology there is a strong need for handling ever smaller amounts of analyte and tendency for increasing the sensitivity to the single-molecule level. Therefore, in photon-starved applications, where single-photon counting detectors are used, it is imperative to develop real-time techniques that can handle discrete sequences of photon counts. Here, the so-called rapid-lifetime determination (RLD) method has been proposed in the past.⁴ In RLD, the fluorescence counts are binned into two adjacent time windows following the laser pulse. The ratio of photon counts in the two time windows is used to calculate the fluorescence lifetime. While RLD is very accurate for large

count rates (on the order of 10^4 s^{-1}), it encounters serious problems for lower count rates, since divisions by zero are encountered with increasing probability.⁵

We present an alternative approach to realtime lifetime determination, which is based on the fact that for a single-exponential decay, the fluorescence lifetime is equal to the average time lag between an excitation laser pulse and the subsequent detection of a fluorescence photon. For each photon, a time-to-amplitude converter (TAC) generates a pulse of an amplitude proportional to the time lag between fluorescence photon and excitation pulse. The resulting sequence of pulses, with exponentially distributed amplitudes and inter-pulse times, is then subjected to a count rate independent averaging procedure. Using Monte Carlo simulations we show that at low count rates, the proposed method excels over RLD.

The lifetime of a single-exponential fluorescence decay is equivalent to the average time lag between excitation pulse and fluorescence photon. We propose two count-rate independent ways of time averaging the TAC output pulse sequence: (i) A fast analog to digital converter (ADC) can be used to digitize the pulse amplitudes and store them in a first-in–first-out (FIFO) memory for subsequent averaging, (ii) averaging can also be achieved by conversion of the pulse sequence into a continuous step function and subsequent low-pass filtering.

If method (ii) is to be applied, the conversion of the pulse sequence into a step function prior to averaging is mandatory because time averaging a function $s_p(t)$, which is a pulse train, will yield proportionality both to the average count rate $\langle f \rangle$ and the average pulse amplitude $\langle a \rangle$, since the integral over the function increases with the number of pulses per unit time: $\langle s_p(t) \rangle = 1/T \int_0^T s_p(t) dt \propto \langle f \rangle \langle a \rangle$. For a step function, this problem is eliminated, since the signal is continuously present, irrespective of the count rate.

Generation of the continuous step-function $s_c(t)$ is accomplished by sampling the voltage level of each TAC pulse and maintaining it until the arrival of the next pulse. In Fig. 1(a), both an experimental pulse sequence (upper trace) and

^{a)}Electronic mail: wtrabe@phys.chem.ethz.ch

^{b)}Present address: Institute of Physics, University of Basel, CH-4056 Basel, Switzerland.

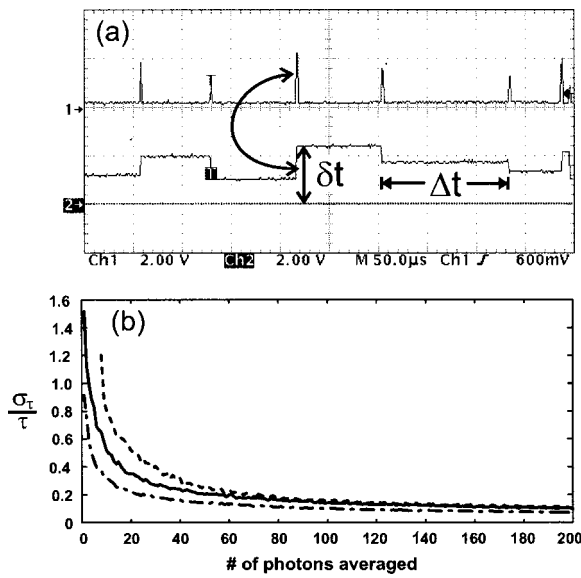


FIG. 1. (a) Illustration of the conversion process from the stochastic pulse sequence into a continuous signal at the example of experimentally measured data. At the arrival of each TAC-pulse, its voltage level is sampled and maintained until the next pulse, as is seen at the lower trace. (b) Monte-Carlo simulations of the experimental noise σ_τ/τ for the RLD method (dashed), the implemented scheme (i) (solid), and an optimal FIFO averager scheme (ii) (dash-dotted).

the corresponding step function (lower trace) before filtering are shown. This type of signal treatment is not entirely equivalent to averaging the amplitudes of a number of pulses, as in approach (i). The stochastic interphoton times lead to varying step widths, giving rise to fluctuating statistical weights for each individual photon. In the following, we will show by analytic derivation that this peculiarity does not affect the outcome of the measurement on average, and constitutes a rather minor source of signal noise.

In the weak excitation regime, the time that elapses between the detection of two photons, i.e., the interphoton time, is exponentially distributed. Assuming that a photon was emitted at $t=0$, the temporal probability density for the emission of the next photon at time Δt is given by: $\rho_{ipr}(\Delta t) = f \exp(-f\Delta t)$, where f is the average count rate and Δt is the interphoton time. The distribution of step widths Δt is thus given by $\rho_{ipr}(\Delta t)$. The second quantity that characterizes an individual step is its amplitude, which is proportional to the start-stop time lag. Its values are exponentially distributed as well: $\rho_{em}(\delta t) = (1/\tau) \exp(-(\delta t)/\tau)$, where τ is the fluorescence lifetime. Since Δt and δt are statistically independent, the two-dimensional probability density $\rho(\Delta t, \delta t)$ for finding a step of length Δt and amplitude δt (see Fig. 1) is given by: $\rho(\Delta t, \delta t) = \rho_{ipr}(\Delta t) * \rho_{em}(\delta t) = f/\tau \exp(-f\Delta t) \exp(-\delta t/\tau)$. The time average of the step-function $s(t)$, corresponding to the low-pass filtered $s(t)$ is given by: $\langle s(t) \rangle = 1/T \int_0^T s(t) dt$, which can be written as a sum over n steps due to n photons emitted in the time interval T : $\langle s(t) \rangle = 1/T \sum_{i=1}^n \delta t_i \Delta t_i$, where the $\delta t_i \Delta t_i$ are the areas of individual steps, and T is the time constant of the averager. Taking into account that the expectation value of the sum over n individual steps equals the n -fold expectation value of one step, we find that: $\langle s(t) \rangle$

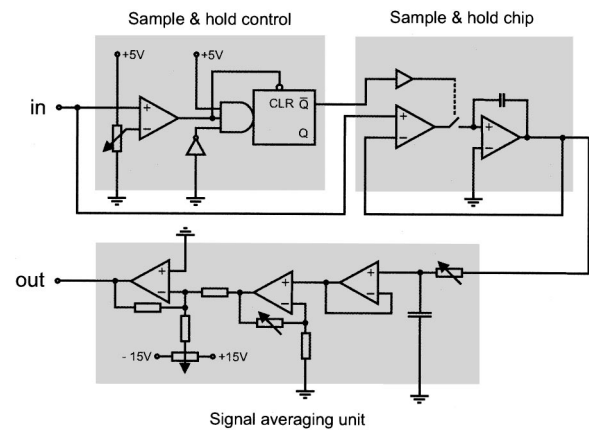


FIG. 2. Sketch of the signal processing electronics consisting of three main units. The sample and hold control, which selects the time window for measurement of the input voltage, the sample and hold chip, and a variable cutoff frequency low-pass filter combined with a final stage for adjustment of offset and gain.

$= n/T \int_0^\infty \int_0^\infty \Delta t \delta t \rho(\Delta t, \delta t) d\delta t d\Delta t = n\tau/fT$. On average, the total time T that passes during the emission of n photons, is n/f , hence $\langle s(t) \rangle = \tau$, as has been anticipated.

The figure of merit for an objective comparison of different lifetime determination schemes is the relative error σ_τ/τ of the lifetime signal as a function of the number n of photons in the observation time window, where σ_τ is the standard deviation of the lifetime signal. In order to evaluate σ_τ/τ for RLD, and the schemes (i) and (ii) proposed here, we implemented a Monte Carlo routine for generating photon sequences obeying $\rho(\Delta t, \delta t)$. For each value of n , we generated 400 sequences containing n photons and carried out the algebraic operations that define RLD, methods (i) and (ii). At a given n , we thus obtain 400 estimates of the lifetime, from which both τ and σ_τ can be determined. Figure 1(b) displays σ_τ/τ as a function of n for all three techniques. Large numbers of photons yield low noise for all three techniques. In the few-photon limit, RLD performs badly, since it involves frequent divisions by zero, which introduce additional noise. The averaging scheme (i) yields the best results, since it assigns equal statistical weights to each photon. Scheme (ii) does not introduce significantly higher noise, in spite of fluctuating statistical weights of the individual photons.

To experimentally demonstrate the feasibility of our concept, we implemented the suggested averaging scheme (ii) because it can be built as a standalone unit from cheap electronic parts. Figure 2 depicts the electronic circuit used for pulse-amplitude averaging. The TAC pulses at the input of the circuit are used to trigger a comparator with a selectable threshold voltage. When triggered, the comparator forces the monostable multivibrator to produce a single negative pulse of fixed length, which can be defined via an external RC network (not shown in Fig. 2). The latter initiates the sampling period of a sample-and-hold chip. After the end of the sampling process, the sampled amplitude of the TAC input pulse is maintained, until the arrival of the subsequent pulse. This results in a step function of the kind shown in Fig. 1(a), lower trace. After averaging the signal by a low-pass filter

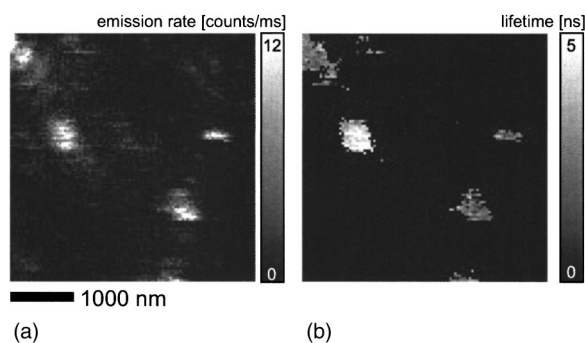


FIG. 3. Simultaneously acquired fluorescence intensity image (a) and lifetime image (b); (a) shows single-molecule spots with varying fluorescence intensities and single-step photobleaching (top-to-bottom scan); (b) only shows pixels for which the intensity in (a) exceeded a preselected threshold. All other pixels are black. Different lifetimes found for the single-molecule spots are indicated by gray levels.

with adjustable cutoff frequency, an inverting amplifier is used for signal amplification and correction of the commonly employed reversed start–stop operation of the TAC. Finally, a further operational amplifier provides the possibility of adding offsets to the output voltage for calibration purposes. For an experimental demonstration, we interfaced our signal processing electronics to an auxiliary analog–digital converter input of a scanning confocal optical microscope (SCOM) to perform single-molecule lifetime imaging.⁶ SCOM is frequently employed for single-molecule microscopy, where low count rates are encountered. Since SCOM is a type of scanning microscopy, real-time image buildup is desired. The SCOM employed in this study is a sample-scanning SCOM equipped with a single-photon counting avalanche photodiode (SPAD). An actively mode-locked Nd:YAG laser (Coherent Antares), frequency doubled to 532 nm is used as a light source that delivers circularly polarized 100 ps pulses with a repetition rate of 76 MHz. The TAC employed (Nuclear Enterprises, NE 4645) has a range of 50 ns. The sample is prepared by codissolving appropriate concentrations of 1,1'-dioctadecyl-3,3,3',3'-tetramethylindocarbocyanine (DiI) with PMMA in toluene and spin casting it onto cover slides. The cover slides were baked at 510 °C for 5 h to remove organic contaminants. Examination of the polymer film by atomic force microscopy revealed a smooth film with a uniform thickness of 30 nm. Figure 3 shows simultaneously recorded fluorescence inten-

sity (a) and lifetime (b) images. Each fluorescence spot in (a) corresponds to a single chromophore. Some fluorescence spots in (a) are partially cut off due to discrete photobleaching. In the lifetime image (b), only those pixels of the image are displayed, for which the fluorescence intensity in (a) significantly exceeds the background count rate. This is commonly done in lifetime imaging, since the signal shows excessive fluctuations in low count-rate regions of the image, rendering the relevant features indiscernible. In image (a), two fluorescent spots of roughly equal intensity are prominent. Inspection of image (b) shows clearly distinct lifetimes for the two fluorescence spots. The fact that lifetime differences between molecules of one and the same species are observed is a result of the immediate vicinity of the polymer–air interface.⁷ Depending on the relative orientation of the molecule to the interface, the total power that can be radiated by the molecule varies because the nonradiative field components around the molecular dipole interact with the interface. This gives rise to modified fluorescence lifetimes. While molecules with emission dipole moments coplanar to the boundary exhibit lifetimes close to 2 ns, orthogonal orientation results in values around 5 ns. This difference is clearly resolved by our electronics, as seen in Fig. 3(b).

In conclusion, we demonstrated a technique for fluorescence lifetime measurements, which, in spite of its simplicity, achieves a performance comparable to that of costly digital devices. We therefore believe that it is a useful tool for real-time fluorescence lifetime measurements in low count-rate applications.

The authors acknowledge M. Kreiter, M. Prummer, and B. Sick for helpful discussions. The project was funded by ETH Zurich.

¹J. R. Lakowicz, *Principles of Fluorescence Spectroscopy* (Plenum, New York, 1983).

²D. O'Connor and D. Philips, *Time-Correlated Single-Photon Counting* (Academic, London, 1984).

³P. C. Schneider and R. M. Clegg, *Rev. Sci. Instrum.* **68**, 4107 (1997).

⁴K. K. Sharman, A. Periasamy, H. Ashworth, J. N. Demas, and N. H. Snow, *Anal. Chem.* **71**, 947 (1999).

⁵R. M. Ballew and J. N. Demas, *Anal. Chem.* **61**, 30 (1989).

⁶P. Tinnefeld, D. P. Herten, and M. Sauer, *J. Phys. Chem. A* **105**, 7989 (2001).

⁷J. J. Macklin, J. K. Trautman, T. D. Harris, and L. E. Brus, *Science* **272**, 255 (1996).